# The role of tumor necrosis factor receptor superfamily molecules on regulation of T cell response to Zika virus

Rebecca Salgado

Advisors: Dr. Kristopher Koudelka[1] and Dr. Sujan Shresta[2]

Committee members: Dr. Dawne Page[1] and Dr. Ying-Ting Wang[2]

[1]Biology Department, Point Loma Nazarene University, San Diego, California, 92106

[2]Division of Inflammation Biology, La Jolla Institute for Immunology, La Jolla, California 92037

**Abstract**:

Zika virus (ZIKV) is a member of the *Flaviviridae* virus family and as of February 2016 has been declared a global public health emergency by the World Health Organization. Understanding the T cell response to ZIKV is critical in making steps towards developing vaccines and antiviral therapies. This project investigated the effect of tumor necrosis factor receptor (TNFR) superfamily members on T cell activation during a primary ZIKV infection. The T cell response was most aptly seen in wild-type C57BL/6J mice treated with an anti-Ifnar1 blocking antibody one day prior to infection. Expression levels of multiple TNFR superfamily members (BAFFR, CD30, ICOS, OX40, 4-1BB, CD27, GITR, and TNFR1) in both naïve and antigen specific T cells were analyzed over a variety of infection timepoints. In particular, expression levels of ICOS, GITR, and OX40 were higher in antigen-specific $CD4^+$ and $CD8^+$ T cells than naïve T cells at 5 days post infection. In terms of T cell kinetics of WT C57BL/6J mice treated with agonistic anti-OX40, anti-GITR, anti-OX40 and anti-GITR (combination), and isotype control antibody treatments 7 days post infection, there was a difference in the production of Granzyme B in antigen-specific $CD8^+$ T cells in mice treated with agonistic anti-GITR and the combination agonistic anti-OX40 and anti-GITR antibody treatments. These findings warrant further study into the potential impact engaging OX40 and GITR could have on T cell response to ZIKV.

**Introduction:**

Zika virus (ZIKV) is a single-stranded RNA arbovirus in the same family as other mosquito-borne viruses such as Yellow Fever, West Nile, and Dengue [1]. ZIKV was first isolated from a sentinel monkey in the Zika Forest of Uganda in 1947 and was isolated from *Aedes africanus* mosquitos in 1948[2]. The primary vector route for virus transmission is the bite of an infected female *Aedes aegypti* mosquito [3], though the virus can also be transmitted through other non-vector routes such as vertical (mother to infant) [4] and sexual transmission [5]. The first major outbreak of ZIKV occurred in 2007 on the Yap Island of the Federal States of Micronesia, where 73% of the population 3 years of age and older was infected [6]. In 2013, a second major outbreak occurred in French Polynesia [7]. Since 2015, ZIKV has been reported in 67 countries and territories in the Oceania region and the Americas [8]. The rise of ZIKV has also been associated with increased cases of ZIKV-associated infant microcephaly; from November 2015 through July 2016, Brazil reported that 15.4% of confirmed microcephaly cases were found to be ZIKV-associated [9]. Additionally, in 2015 the World Health Organization issued an alert regarding the rise in cases of ZIKV-associated Guillain–Barré syndrome (GBS). GBS is characterized by rapid muscle weakness from damages to the peripheral nervous system during an immune response [10]. The number of reported ZIKV cases and ZIKV-associated neurological pathologies led the World Health Organization to declare ZIKV a global public health emergency in 2016, making the effort to develop a vaccine or anti-viral therapies more critical than ever.

The tumor necrosis factor receptor (TNFR) superfamily members are expressed on immune and non-immune cells. Together with their ligands, TNFR superfamily members provide cell communication signals for multiple cell types, including skin, bone, and lymphoid

organs [11]. Once the ligand binds to its receptor, TNFR superfamily members cluster together and transmit signals inside the cell for various cellular processes [12]. TNFR superfamily members have been implicated in autoimmune diseases including rheumatoid arthritis [13], Sjögren's syndrome [14] [15], and irritable bowel disease [16]. Furthermore, TNFR superfamily members such as CD27 [17], OX40 [17] [18] [19], and 4-1BB [19] [20] have been targets for cancer immunotherapy. Certain members of the TNFR superfamily, including GITR, OX40, HVEM, DR3, 4-1BB, CD30 and TNFR2, are implicated in adaptive immune responses and are responsible for costimulatory or coinhibitory signals to T cells [12]. The TNFR superfamily ligands are typically expressed on antigen presenting cells, while the TNFR superfamily receptors are expressed on T cells [21]. In the context of viral infections, TNFR superfamily members initiate a variety of responses including caspase-induced apoptosis, co-stimulation of the canonical NF-κB pathway, and inflammation [22].

TNFR superfamily members have been studied in the context of numerous viruses including HIV [23] [24], hepatitis C [25] [26], and herpesvirus [22] [27] [28] [29]. However, the role of TNFR superfamily members in acute viral infections, specifically for flaviviruses, has yet to be investigated. The goal of this project was to characterize what TNFR superfamily members were expressed during different timepoints of a primary ZIKV infection. Wild-type C57BL/6J, wild-type C57BL/6J treated with an anti-Ifnar1 blocking antibody, and human STAT2 knock-in (*huSTAT2* KI) mouse models were tested to determine which model would best show the expression of TNFR superfamily members and the T cell response after ZIKV infection. The expression levels of TNFR superfamily members were analyzed at 0, 3, 5, 7, and 9 days post infection in both naïve and antigen-specific T cells isolated from splenocytes. The wild-type C57BL/6J mice treated with an anti-Ifnar1 blocking antibody proved to be the most effective model for observing T cell response, with differences in expression of TNFR superfamily members OX40 and GITR pronounced between naïve and antigen-specific T cells. The cytokine production 7 days post infection of wild-type C57BL/6J mice treated with agonistic anti-GITR and anti-OX40 antibodies was also investigated; a significant difference was seen in the production of Granzyme B between mice treated with agonistic anti-GITR and the combination anti-OX40 and anti-GITR antibody treatment in antigen-specific $CD8^+$ T cells compared to the isotype control treated mice. Findings from this project indicate OX40 and GITR are implicated in the primary T cell response to ZIKV, though further investigation needs to be done regarding their specific role in survival and influence of cytokine production.

## Results

### Expression pattern of TNFR superfamily members at 5 dpi in WT C57BL/6J mice, *huSTAT2* KI mice, and WT C57BL/6J mice treated with anti-Ifnar1 blocking antibody

Different mouse models were tested to determine the best model for observing expression changes in TNFR superfamily members. Wild-type (WT) C57BL/6J mice were infected with ZIKV (strain SD001, $1 \times 10^5$ FFU/mouse, intra-footpad route) and expression levels for TNFR superfamily members BAFFR, CD30, ICOS, OX40, 4-1BB, CD27, GITR, and TNFR1 in $CD4^+$ and $CD8^+$ T cells were determined 0, 5, and 7 days post infection (dpi) (**Figure 1**). Testing the human STAT2 knock-in (*huSTAT2* KI) model was based on prior research showing ZIKV

antagonizes the human interferon pathway by degrading the signal transducer and activator of transcription 2 (STAT2) protein [30] [31]. However, ZIKV does not antagonize the murine STAT2 protein [30], and thus does not effectively inhibit the murine interferon response. *huSTAT2* KI mice were infected with ZIKV (strain SD001, $1 \times 10^5$ FFU/mouse, intra-footpad route) and expression levels for TNFR superfamily members CD30, ICOS, OX40, 4-1BB, CD27, GITR, and TNFR1 in $CD4^+$ and $CD8^+$ T cells were determined 0, 3, 5, and 7 days post infection (dpi) (**Figure 2**). There was a shift in ICOS expression between naïve and antigen-specific $CD4^+$ T cells in both the WT C57BL/6J and *huSTAT2* KI models; other superfamily members had minimal to no shifts in expression between naïve and antigen-specific $CD4^+$ and $CD8^+$ T cells in both the WT C57BL/6J and *huSTAT2* KI model.

The next model tested was WT C57BL/6J mice treated with an anti-Ifnar1 blocking antibody one day prior to infection (dose of 1 mg/mouse, intraperitoneal (I.P.) route) and infected the following day with ZIKV (strain SD001, $1 \times 10^3$ FFU/mouse, intra-footpad route). Expression for TNFR superfamily members BAFFR, CD30, ICOS, OX40, 4-1BB, CD27, GITR, and TNFR1 in $CD4^+$ and $CD8^+$ T cells was determined 0, 3, 5, 7, and 9 days post infection (dpi); only data from day 5 is shown (**Figure 3**). Comparing the expression levels between the TNFR superfamily members tested in both $CD4^+$ and $CD8^+$ T cells, the shift in TNFR superfamily member expression was best seen using the WT C57BL/6J mice treated with an anti-Ifnar1 blocking antibody one day prior to infection (**Figure 4**).

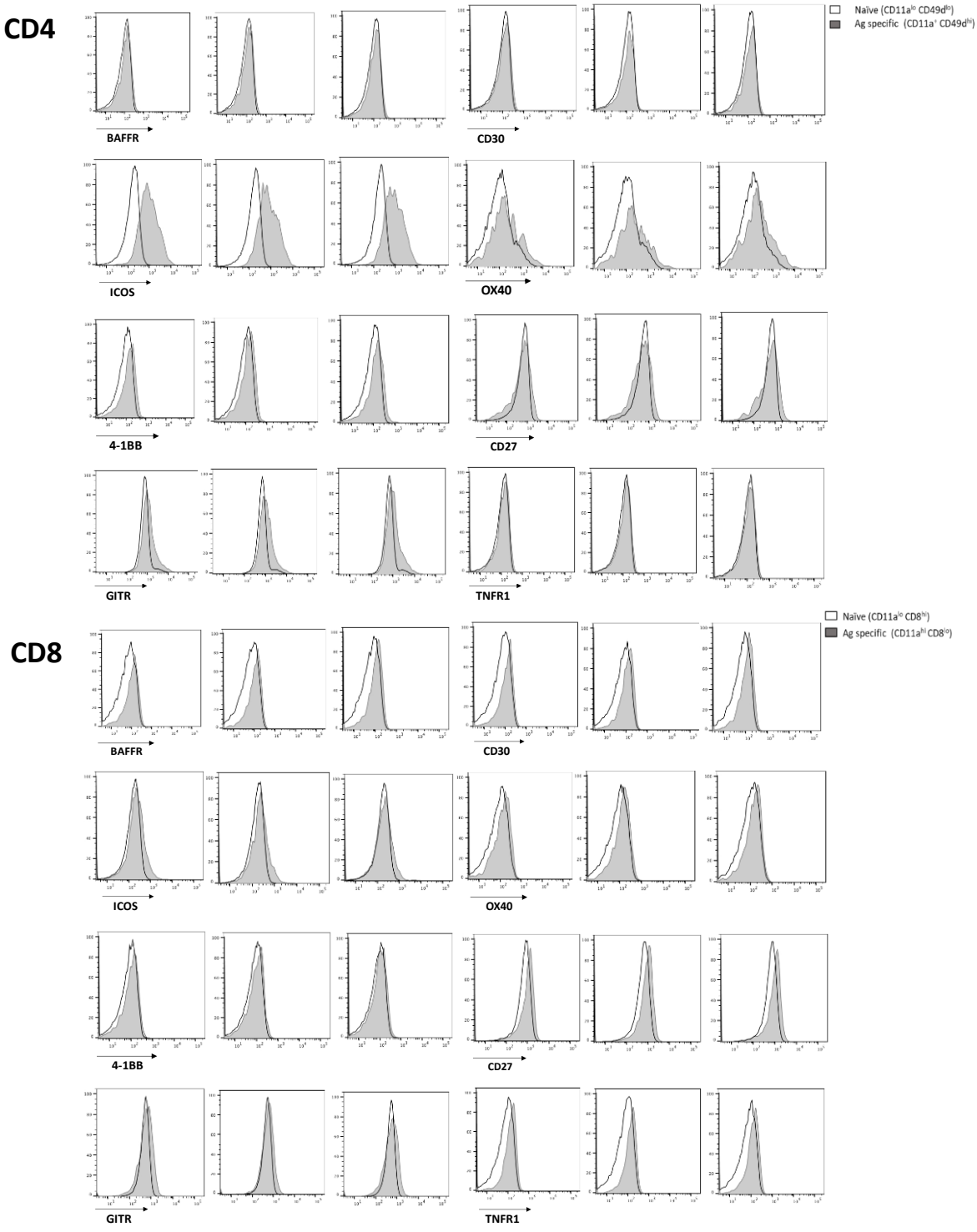


**Figure 1: Expression patterns in TNFR superfamily members 5 days post infection in WT C57BL/6J mice.**

WT C57BL/6J mice were infected with $10^5$ Focus Forming Units (FFU) of ZIKV (strain SD001). Expression levels of TNFR superfamily members in naïve and antigen-specific $CD4^+$ and $CD8^+$ T cells were collected at 0 (n=3), 5 (n=3), and 7 (n=3) days post infection (dpi); only data from 5 dpi is shown.

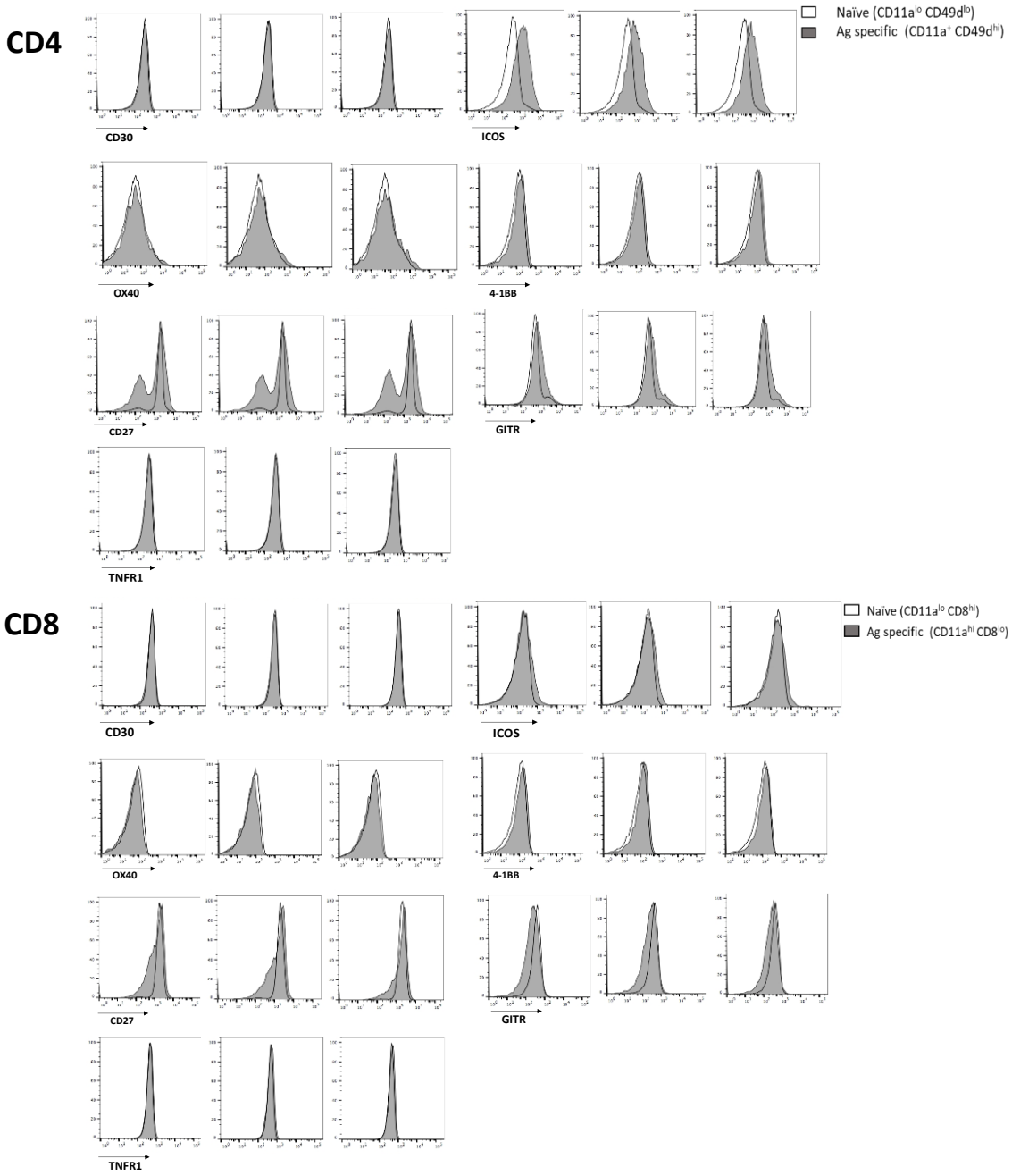


**Figure 2: Expression patterns in TNFR superfamily members 5 days post infection in *huSTAT2* KI mice.**

*huSTAT2* KI mice were infected with $10^5$ Focus Forming Units (FFU) of ZIKV (strain SD001). Expression levels of TNFR superfamily members in naïve and antigen-specific $CD4^+$ and $CD8^+$ T cells were collected at 0 (n=2), 3 (n=4), 5 (n=5), and 7 (n=5) days post infection (dpi); only data from 3 replicates at 5 dpi is shown.

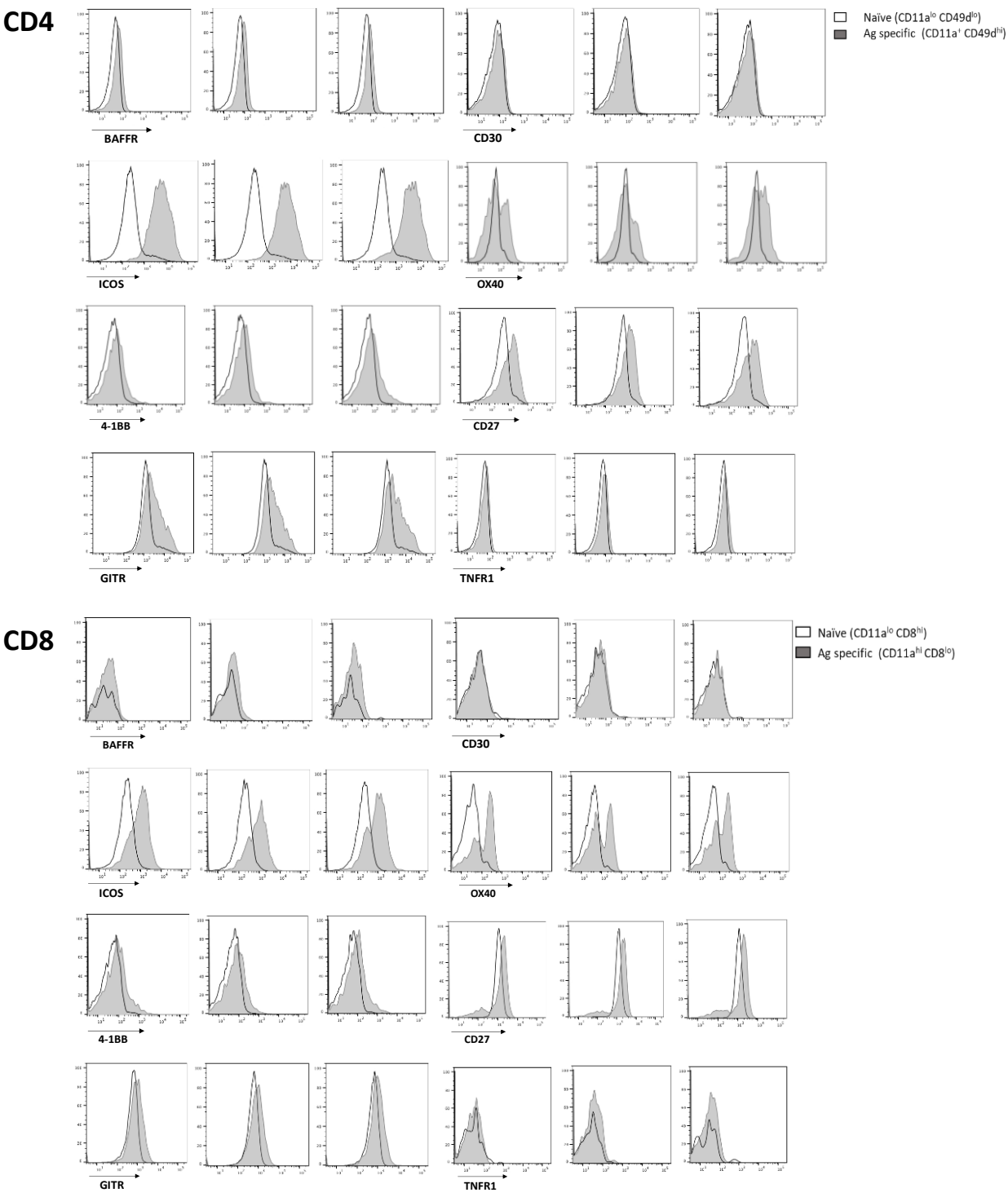


**Figure 3: Expression patterns in TNFR superfamily members 5 days post-infection in WT C57BL/6J mice treated with an anti-Ifnar1 blocking antibody.**

WT C57BL/6J mice were treated with 1 mg of anti-Ifnar1 blocking antibody one day prior to infection. The following day, mice were infected with $10^3$ Focus Forming Units (FFU) of ZIKV (strain SD001). Expression levels of TNFR superfamily members in naïve and antigen-specific $CD4^+$ and $CD8^+$ T cells were collected at 0 (n=3), 3 (n=3), 5 (n=3), 7 (n=3), and 9 (n=3) days post infection (dpi); only data from 5 dpi is shown.

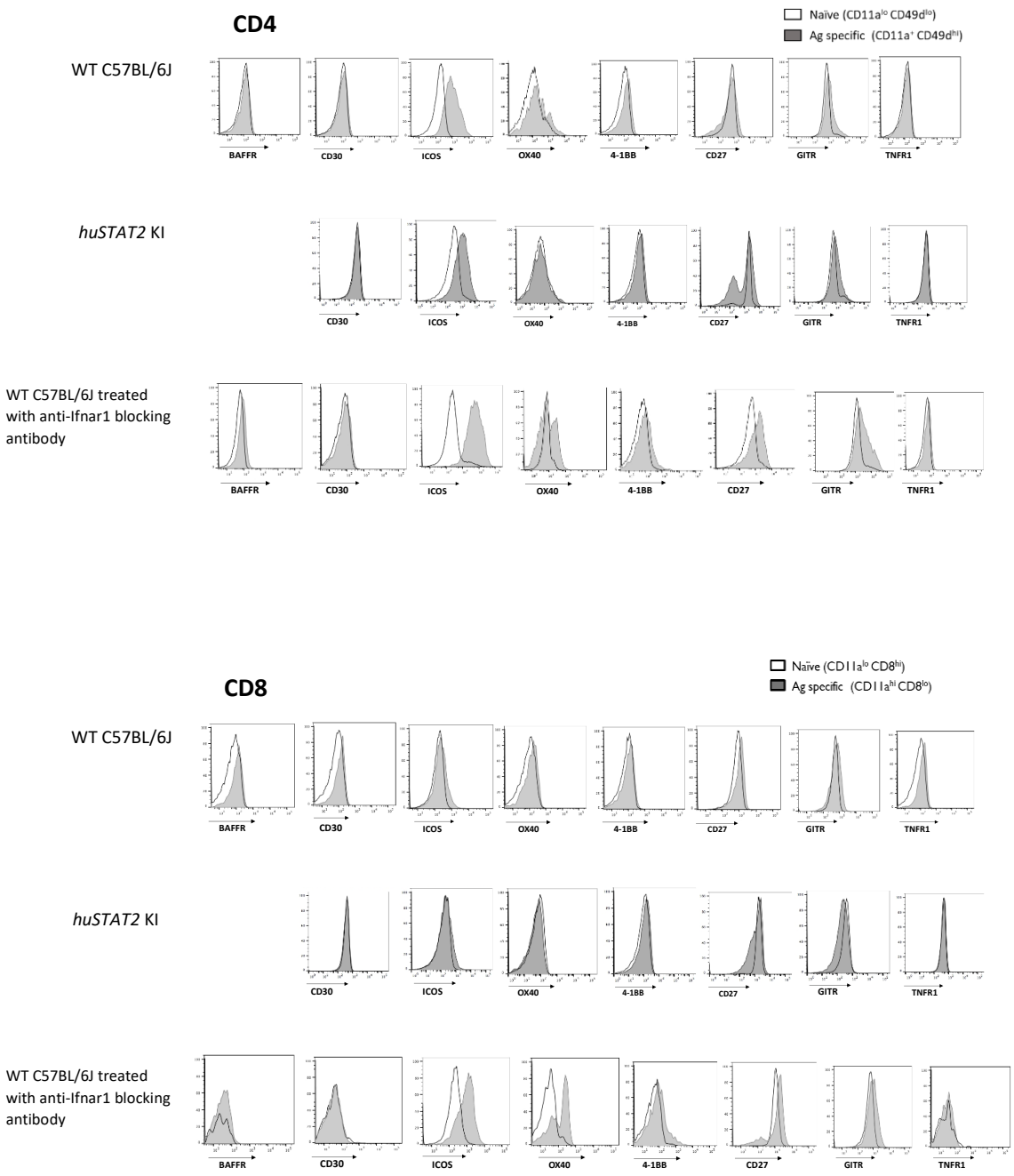


**Figure 4: Comparing expression levels of TNFR superfamily members in WT C57BL/6J, *huSTAT2* KI, and anti-Ifnar1 blocking antibody treated WT C57BL/6J mice.**
WT C57BL/6J and *huSTAT2* KI mice were infected with $10^5$ Focus Forming Units (FFU) of ZIKV (strain SD001). In a separate model, WT C57BL/6J mice were treated with an anti-Ifnar1 blocking antibody (1 mg) one day prior to infection and were infected the following day with $10^3$ FFU of ZIKV (SD001). Expression levels of BAFFR, CD30, ICOS, OX40, 4-1BB, CD27, GITR, and TNFR1 in naïve and antigen-specific T cells at 5 days post infection (dpi) are shown (only 1 replicate shown per model). Note: BAFFR was not tested for in the *huSTAT2* KI model.

**The number of $CD4^+$ and $CD8^+$ antigen-specific T cells that express OX40 and GITR increase at 5 and 7 days post infection**

Since the WT C57BL/6J mice treated with an anti-Ifnar1 blocking antibody showed the most prominent shift in expression of TNFR superfamily members in both naïve and antigen-specific $CD4^+$ and $CD8^+$ T cells, the number of $CD4^+$ and $CD8^+$ T cells expressing the TNFR superfamily members tested was considered in this model. The number of antigen-specific $CD4^+$ T cells at 5 days post infection (dpi) for BAFFR, ICOS, OX40, CD27, GITR, and TNFR1 increased significantly ($p = 0.0357$) compared to 0 dpi (**Figure 5**). At 7 dpi, the number of antigen-specific $CD4^+$ T cells for BAFFR, CD30, ICOS, OX40, CD27, GITR, and TNFR1 increased significantly ($p = 0.0357$) when compared to 0 dpi. For $CD8^+$ T cells, the number of antigen-specific T cells expressing ICOS, OX40, 4-1BB, CD27, and GITR also had a significant increase ($p = 0.0357$) at 5 dpi (**Figure 5**). Antigen-specific $CD8^+$ T cells expressing ICOS, OX40, 4-1BB, CD27, and GITR at 7 dpi also had an increase in number when compared to 0 dpi ($p = 0.0357$) (**Figure 5**). These results indicate that the peak response of $CD4^+$ and $CD8^+$ antigen-specific T cells that express TNFR superfamily members was at 7 days post infection. Additionally, these results show an increase in the number of antigen-specific T cells for both $CD4^+$ and $CD8^+$ T cells expressing the TNFR superfamily members ICOS, OX40, and GITR. Based on the results from TNFR superfamily member expression at 5 dpi (**Figure 3**) and the increase in both $CD4^+$ and $CD8^+$ antigen-specific T cells, OX40 and GITR were the TNFR superfamily members of interest for the remainder of the project.

**CD4**

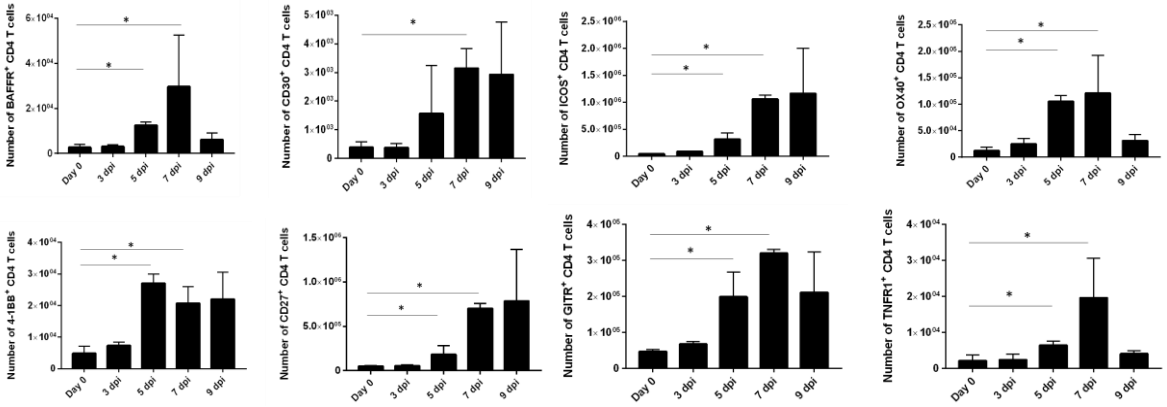


**CD8**

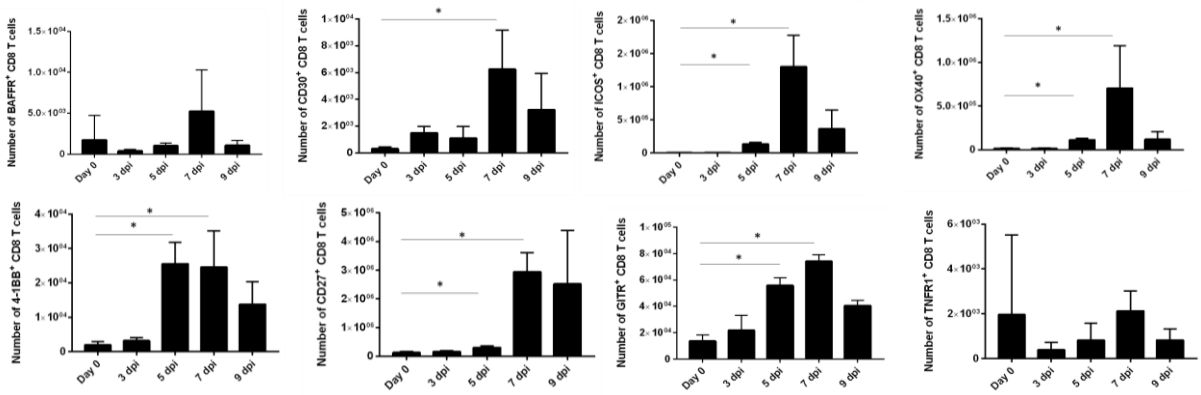


**Figure 5: Number of antigen-specific CD4$^+$ and CD8$^+$ T cells expressing TNFR superfamily members in WT C57BL/6J mice treated with an anti-Ifnar1 blocking antibody.**
One day prior to infection with $10^5$ Focus Forming Units (FFU) of ZIKV strain SD001, WT C57BL/6J were treated with an anti-Ifnar1 blocking antibody. Five different timepoints were tested: 0 (n=5), 3 (n=3), 5 (n=3), 7 (n=3), and 9 (n=3) days post infection (dpi). Shown is the number of antigen-specific CD4$^+$ and CD8$^+$ T cells expressing BAFFR, CD30, ICOS, OX40, 4-1BB, CD27, GITR, and TNFR1. A non-parametric Mann-Whitney test was used to compare 0 and 5 dpi, as well as 0 and 7 dpi. Significance difference (*) was defined by a p value $< 0.05$ and all error bars correspond to SEM.

**Kinetics of the ZIKV-specific $CD4^+$, $CD8^+$, and Tfh T cell response in WT C57BL/6J mice**

To elucidate the effect of OX40 and GITR on the kinetics of the splenic $CD4^+$, $CD8^+$, and Tfh T cell response induced by ZIKV-specific peptides, WT C57BL/6J mice were treated with agonistic anti-OX40, anti-GITR, both anti-OX40 and anti-GITR (combination), or isotype control antibody treatments after infection with ZIKV. For $CD4^+$ T cells stimulated with ZIKV-specific peptide $NS4B_{2480-2494}$, the percentage of antigen-specific $IFN\gamma^+CD4^+$ and $IFN\gamma^+TNF\alpha^+CD4^+$ T cells was higher in the isotype control group than the combination group ($p = 0.0286$) (**Figure 6A**). Additionally, the percentage of antigen-specific $IL\text{-}2^+CD4^+$, $TNF\alpha^+CD4^+$, and $IFN\gamma^+IL\text{-}2^+CD4^+$ T cells was higher in the isotype control group than the anti-OX40 group and the combination group ($p = 0.0286$) (**Figure 6A**). In relation to the total number of splenocytes, there was only a significant difference in the number of antigen-specific $IFN\gamma^+IL\text{-}2^+CD4^+$ T cells, which was higher in the isotype control group compared to the anti-GITR group ($p = 0.0286$) (**Figure 6B**). Similarly, in $CD4^+$ T cells stimulated with ZIKV-specific peptide $E_{644-658}$, the percentage of antigen-specific $IFN\gamma^+CD4^+$, $IL\text{-}2^+CD4^+$, and $IFN\gamma^+IL\text{-}2^+CD4^+$ T cells was higher in the isotype control group than the anti-OX40 group and combination group ($p = 0.0286$) (**Figure 6A**). The percentage of antigen-specific $TNF\alpha^+CD4^+$ and $IFN\gamma^+TNF\alpha^+CD4^+$ T cells was higher in the isotype control group than the anti-OX40 group, anti-GITR group, and combination group ($p = 0.0286$) (**Figure 6A**). For the total number of splenocytes, the number of antigen-specific $IL\text{-}2^+CD4^+$ and $IFN\gamma^+TNF\alpha^+CD4^+$ T cells was higher in the isotype control group compared to the anti-GITR group, while the number of $IFN\gamma^+IL\text{-}2^+CD4^+$ T cells was higher in the isotype control group than the combination group ($p = 0.0286$) (**Figure 6B**). Additionally, the number of antigen-specific $TNF\alpha^+CD4^+$ T cells was higher in the isotype control group compared to the combination and anti-GITR group ($p = 0.0286$) (**Figure 6B**).

For $CD8^+$ T cells stimulated with ZIKV-specific peptide $E_{294-302}$ there was a higher percentage of antigen-specific Granzyme $B^+CD8^+$ T cells in the anti-GITR group and combination group than the isotype control group ($p = 0.0286$) (**Figure 7A**). Additionally, for $CD8^+$ T cells stimulated with $E_{294-302}$ there was a higher percentage of antigen-specific $IFN\gamma^+CD8^+$, $TNF\alpha^+CD8^+$, and $IFN\gamma^+TNF\alpha^+CD8^+$ T cells in the isotype control group than the anti-OX40 group and combination group ($p = 0.0286$) (**Figure 7A**). In terms of the total number of splenocytes, the number of $IFN\gamma^+GranzymeB^+CD8^+$ T cells was higher in the isotype control group than the anti-OX40 and combination group ($p = 0.0286$) (**Figure 7B**). In $CD8^+$ T cells stimulated with ZIKV-specific peptide $NS5_{2783-2792}$, there was a higher percentage of antigen-specific Granzyme $B^+CD8^+$ T cells in the anti-GITR group and combination group than the isotype control group ($p = 0.0286$) (**Figure 7A**). Furthermore, there was a higher percentage of antigen-specific $IFN\gamma^+CD8^+$, $TNF\alpha^+CD8^+$, and $IFN\gamma^+TNF\alpha^+CD8^+$ T cells in the isotype control group than the anti-OX40 group and combination group ($p = 0.0286$) (**Figure 7A**). The number of antigen-specific Granzyme $B^+CD8^+$ T cells was higher in the combination group compared to the isotype control group ($p = 0.0286$) (**Figure 7B**). For antigen-specific $IFN\gamma^+CD8^+$, $TNF\alpha^+CD8^+$, and $IFN\gamma^+TNF\alpha^+CD8^+$ T cells, the number of cells was higher in the isotype control group compared to the combination and anti-OX40 group ($p = 0.0826$) (**Figure 7B**).

Splenocytes were also analyzed for the Tfh T cell response; the percentage (**Figure 8A**) and number (**Figure 8B**) of antigen-specific $CD4^+CD44^+CXCR5^+PD\text{-}1^+$ in the anti-OX40 group, anti-GITR group, and combination group was not significant compared to the isotype control group.

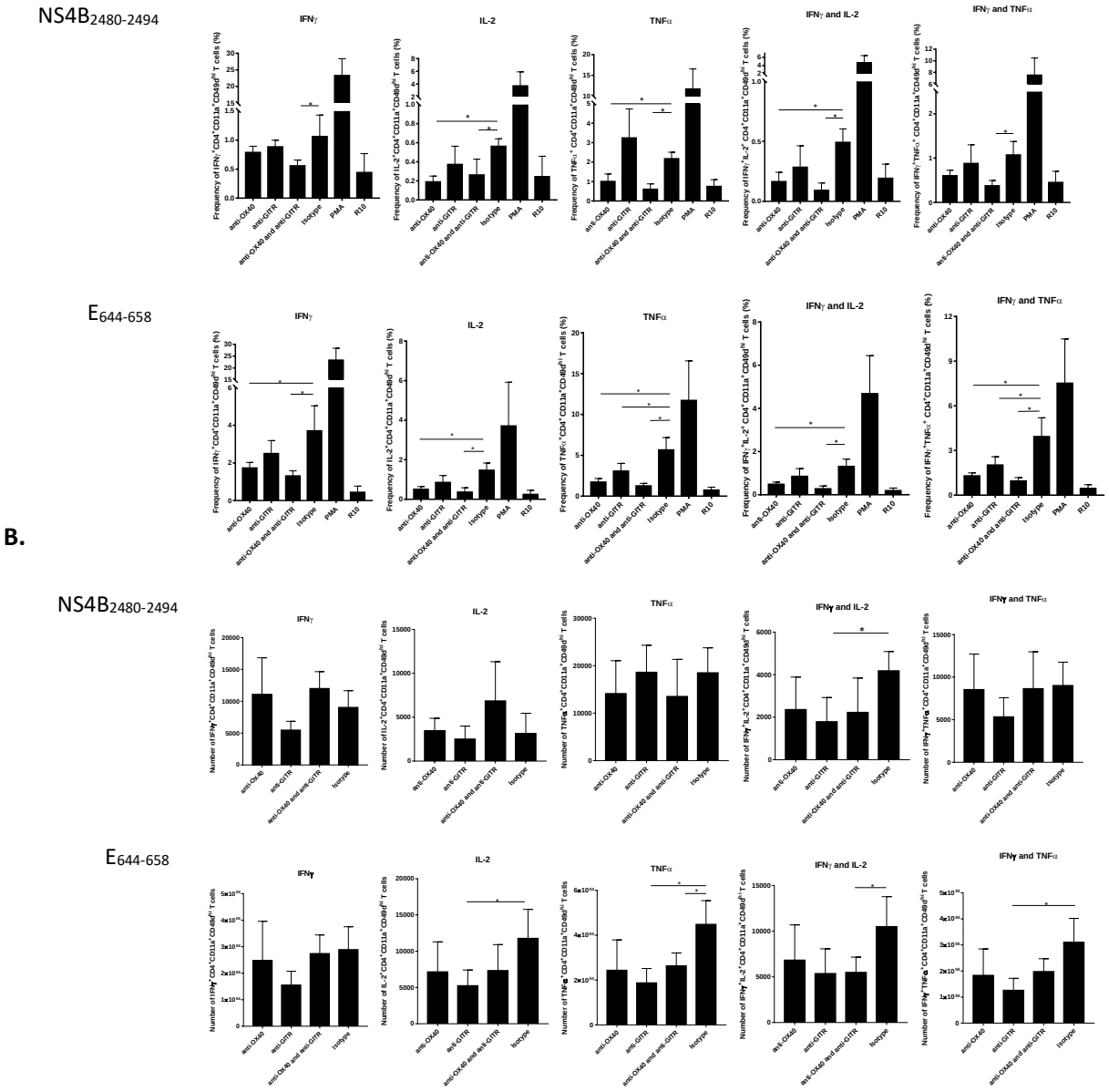


**Figure 6: T cell kinetics of CD4⁺ T cells in WT C57BL/6J mice treated with agonistic anti-OX40 and/or agonistic anti-GITR antibody treatments 7 days post infection.**

4 groups of WT C57BL/6J mice were infected with $10^5$ Focus Forming Units (FFU) of ZIKV strain SD001. Two hours after infection, mice were treated with either agonistic anti-OX40 (200 µg/mouse, n = 4), agonistic anti-GITR (200 µg/mouse, n = 4), both agonistic anti-OX40 and anti-GITR (100 µg of each antibody/mouse, n = 4), or isotype controls (100 µg of each isotype/mouse, n = 4). Spleens were collected 7 days post infection and the splenocytes isolated, stimulated with ZIKV-specific peptides $NS4B_{2480-2494}$ or $E_{644-658}$ or a stimulation cocktail of PMA (positive control, data not shown) and stained for intracellular cytokines. **A**) Frequency of antigen-specific $IFN\gamma^+CD4^+$, $IL\text{-}2^+CD4^+$, $TNF\alpha^+CD4^+$, $IFN\gamma^+IL\text{-}2^+CD4^+$, and $IFN\gamma^+TNF\alpha^+CD4^+$ T cells stimulated with either ZIKV-specific peptides $NS4B_{2480-2494}$ or $E_{644-658}$. **B**) Number of antigen-specific $IFN\gamma^+CD4^+$, $IL\text{-}2^+CD4^+$, $TNF\alpha^+CD4^+$, $IFN\gamma^+IL\text{-}2^+CD4^+$, and $IFN\gamma^+TNF\alpha^+CD4^+$ T cells stimulated with either ZIKV-specific peptides $NS4B_{2480-2494}$ or $E_{644-658}$. A non-parametric Mann-Whitney teste was used to compare the anti-OX40 group to the isotype control, anti-GITR to the isotype control, and the combination (anti-OX40 and anti-GITR) group to the isotype control. Significance difference (*) was defined by a p value < 0.05 and all error bars correspond to SEM.

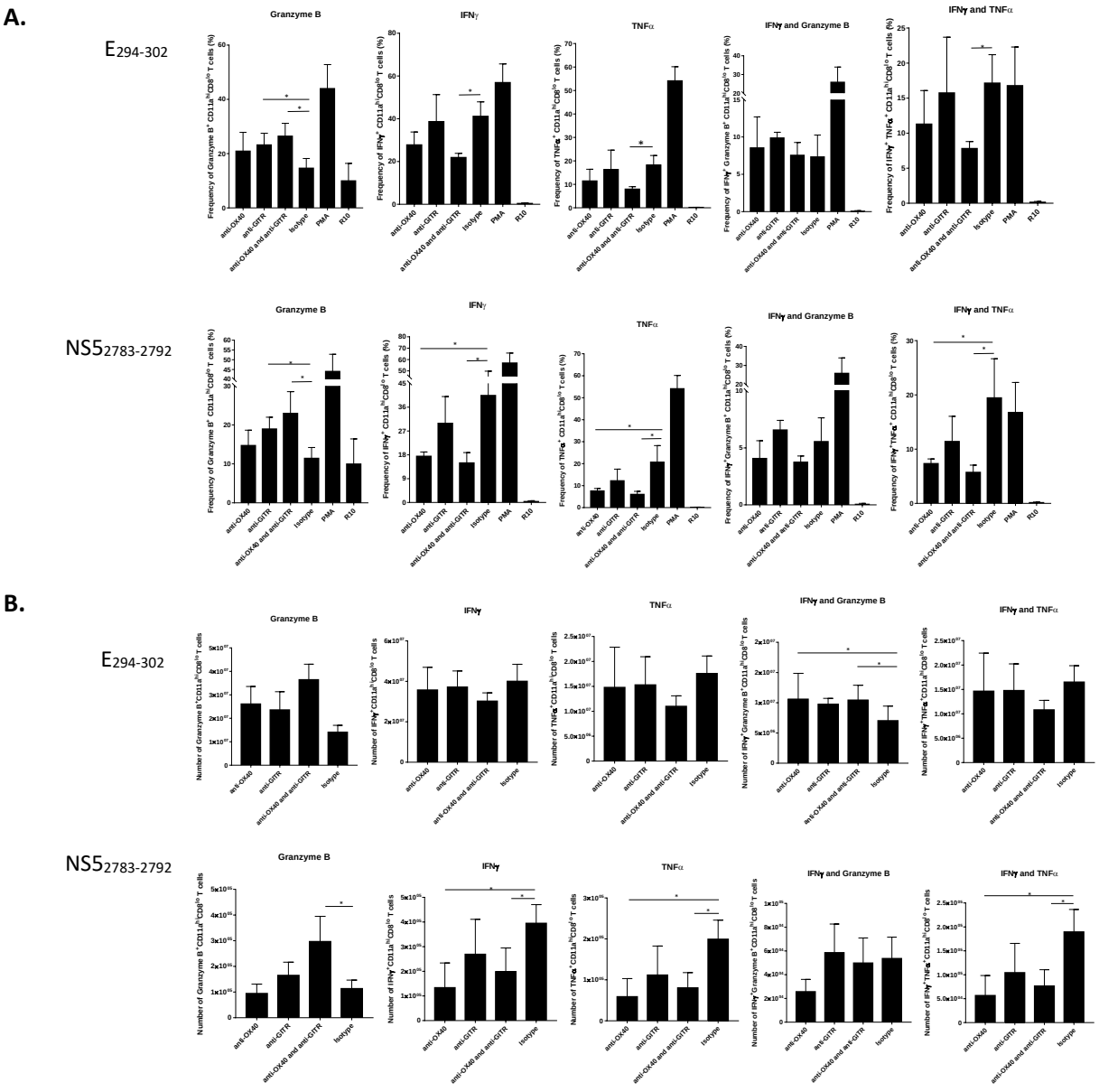


**Figure 7: Splenocyte kinetics of CD8$^+$ T cells in WT C57BL/6J mice treated with agonistic anti-OX40 and/or agonistic anti-GITR antibody treatments 7 days post infection.**

4 groups of WT C57BL/6J mice were infected with $10^5$ Focus Forming Units (FFU) of ZIKV strain SD001. Two hours after infection, mice were treated with either agonistic anti-OX40 (200 µg/mouse, n = 4), agonistic anti-GITR (200 µg/mouse, n = 4), both agonistic anti-OX40 and anti-GITR (100 µg of each antibody/mouse, n = 4), or isotype controls (100 µg of each isotype/mouse, n = 4). Spleens were collected 7 days post infection and the splenocytes isolated, stimulated with ZIKV-specific peptides $E_{294\text{-}302}$ or $NS5_{2783\text{-}2792}$ or a stimulation cocktail of PMA (positive control, data not shown) and stained for intracellular cytokines. **A**) Frequency of antigen-specific Granzyme B$^+$CD8$^+$, IFNγ$^+$CD8$^+$, TNFα$^+$CD8$^+$, IFNγ$^+$GranzymeB$^+$CD8$^+$, and IFNγ$^+$TNFα$^+$CD8$^+$ T cells stimulated with either ZIKV-specific peptides $E_{294\text{-}302}$ or $NS5_{2783\text{-}2792}$. **B**) Number of antigen-specific Granzyme B$^+$CD8$^+$, IFNγ$^+$CD8$^+$, TNFα$^+$CD8$^+$, IFNγ$^+$GranzymeB$^+$CD8$^+$, and IFNγ$^+$TNFα$^+$CD8$^+$ T cells stimulated with either ZIKV-specific peptides $E_{294\text{-}302}$ or $NS5_{2783\text{-}2792}$. A non-parametric Mann-Whitney test was used to compare the anti-OX40 group to the isotype control, anti-GITR to the isotype control, and the combination (anti-OX40 and anti-GITR) group to the isotype control. Significance difference (*) was defined by a p value < 0.05 and all error bars correspond to SEM.

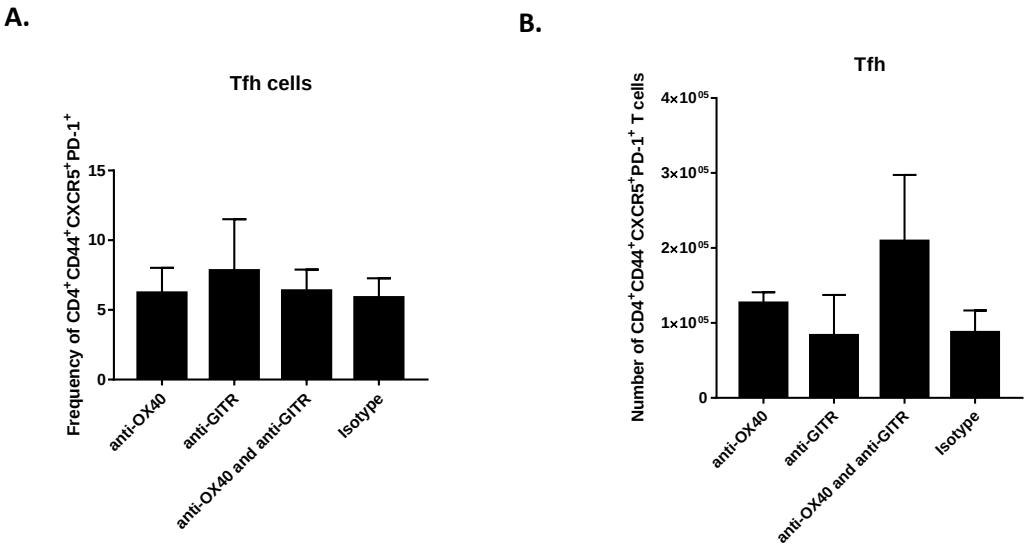


**Figure 8: Splenocyte kinetics in WT C57BL/6J mice treated with agonistic OX86 and/or DTA-1 antibody treatments 7 days post-infection.**

4 groups of WT mice were infected with $10^5$ Focus Forming Units (FFU) of ZIKV strain SD001. Two hours after infection, mice were treated with either agonistic anti-OX40 (200 μg/mouse, n = 4), agonistic anti-GITR (200 μg/mouse, n = 4), both agonistic anti-OX40 and agonistic anti-GITR (100 μg of each antibody/mouse, n = 4), or isotype control (100 μg of each isotype/mouse, n = 4). Spleens were collected 7 days post infection and the splenocytes isolated for extracellular staining of Tfh markers. **A**) Frequency of antigen-specific $CD4^+CD44^+CXCR5^+PD\text{-}1^+$ T cells. **B**) Number of antigen-specific $CD4^+CD44^+CXCR5^+PD\text{-}1^+$ T cells. A non-parametric Mann-Whitney test was used to compare the anti-OX40 group to the isotype control, anti-GITR group to the isotype control, and the combination (anti-OX40 and anti-GITR) group to the isotype control. Significance difference (*) was defined by a p value < 0.05 and all error bars correspond to SEM.

## Discussion

In this study, expression levels of various TNFR superfamily members on both naïve and antigen-specific T cells were characterized after ZIKV infection. Out of the time points tested, the shift in expression of TNFR superfamily members was most prominent at 5 days post infection, while the peak T cell response was at 7 days post infection. The WT C57BL/6J mice treated with an anti-Ifnar1 blocking antibody one day before infection served as the best model to observe changes in both expression of TNFR superfamily members and T cell activation. OX40 and GITR were selected as potential targets to observe the effects of engaging TNFR superfamily members after ZIKV infection. Treatment with agonistic anti-OX40 antibody and/or agonistic anti-GITR antibody after ZIKV infection did not affect the T cell kinetics of $CD4^+$ T cells, the majority of $CD8^+$ T cells or Tfh cells; however, mice treated with an agonistic anti-GITR antibody and a combination of agonistic anti-OX40 and anti-GITR antibodies had a higher frequency of antigen-specific $CD8^+$ T cells that produced Granzyme B.

Based on expression data and the number of antigen-specific $CD4^+$ and $CD8^+$ T cells for each TNFR superfamily member, OX40 and GITR emerged as potential targets to study the effect of engaging TNFR superfamily members during T cell activation. The OX40 receptor was first identified in 1987[32] and the gene for OX40 and other TNFR superfamily members, including GITR, is located on human chromosome 1[33]. OX40 is expressed primarily on activated $CD4^+$ and $CD8^+$ T cells as well as Th2, Th1, and Th17 cells[33]. Many studies have focused on the functional aspect OX40 plays in $CD4^+$ T cells, particularly in terms of cell division and survival. In this study, the number of antigen-specific $CD4^+$ and $CD8^+$ cells expressing OX40 did increase both 5 and 7 days post infection, indicating levels of OX40 expression are changing after ZIKV infection. Also observed was that GITR expression followed the same trend as OX40 in terms of an increase in the number of antigen-specific $CD4^+$ and $CD8^+$ T cells 5 and 7 days post infection. GITR (glucocorticoid-induced tumor necrosis factor receptor-related protein) was first cloned in 1997 in a hybridoma T cell line treated with dexamethasone, where it was discovered to be involved in the regulation of T cell receptor-mediated death [34]. Previous studies have shown GITR is expressed at high levels in both $CD4^+$ and $CD8^+$ T cells after activation[35-37]; results from this study indicate a similar trend in the enhanced expression of GITR after ZIKV infection.

Of the mouse models tested, the WT C57BL/6J mice treated with an anti-Ifnar1 blocking antibody one day prior to infection proved to be the most viable model for observing both expression of TNFR superfamily members and T cell activation. One of the challenges of studying ZIKV in mice is that the virus does not block the murine Type I Interferon response, allowing the murine host cells to prevent viral replication. In humans, ZIKV and other flaviviruses have viral proteases that target host proteins involved in interferon signaling, allowing the virus to escape the host's interferon response [38]. When comparing the WT C57BL/6J model to the WT C57BL/6J mice treated with an anti-Ifnar1 blocking antibody, there was little to no shift in expression of TNFR superfamily members between naïve and antigen-specific $CD4^+$ and $CD8^+$ T cells at 5 days post infection for the WT C57BL/6J. Additionally, prior studies showing that flaviviruses ZIKV and Dengue (DENV) antagonize the human STAT

2 protein[30, 39, 40] made the human STAT2 knock-in (*huSTAT2* KI) model a promising approach. However, there was little to no shift in expression of TNFR superfamily members between naïve and antigen-specific $CD4^+$ and $CD8^+$ T cells at 5 days post infection. These results indicate the WT C57BL/6J and the *huSTAT2* KI show little changes in expression of TNFR superfamily members between naïve and antigen specific $CD4^+$ and $CD8^+$ T cells when compared to the WT C57BL/6J mice treated with an anti-Ifnar1 blocking antibody one day before infection.

To elucidate the effects of engaging OX40 and GITR receptors during T cell activation after ZIKV infection, agonistic antibody treatments for both OX40 and GITR were tested. Agonist antibodies are functional forms of a receptor's natural ligand and have a higher affinity for the targeted receptor than does the natural ligand. Agonist OX40 treatments have been used in a variety of pre-clinical tumor models, including B16 melanoma[41], fibrosarcoma [42], CT26 colon cancer[43], and GL261 glioma[44], to promote an anti-tumor response. In a similar manner, agonist GITR treatments have been used to promote anti-tumor responses in murine tumor models of B16 melanoma[45], CT26 colon cancer [46], and fibrosarcoma[47]. However, little research has been done regarding agonistic antibody treatments and acute flavivirus infections. The T cell kinetics of mice treated with agonistic anti-OX40 and/or anti-GITR antibody treatments were investigated to determine the cytokine profile of $CD4^+$, $CD8^+$, and Tfh T cells. For $CD4^+$ T cells stimulated with ZIKV-specific peptides $NS4B_{2480\text{-}2494}$ or $E_{644\text{-}658}$, there were more antigen-specific cells that produced IFNγ, IL-2, and/or TNFα in the isotype control treated mice than in mice treated with agonistic anti-OX40, agonistic anti-GITR, or both agonistic anti-OX40 and anti-GITR. These results indicate engaging OX40 and GITR in the context of stimulated $CD4^+$ T cells could be hindering cytokine production. For $CD8^+$ T cells stimulated with ZIKV-specific peptide $E_{294\text{-}302}$, there were more antigen-specific cells that produced IFNγ and/or TNFα in the isotype treated mice than mice treated with both agonistic anti-OX40 and anti-GITR (combination group). Similarly, in $CD8^+$ T cells stimulated with ZIKV-specific peptide $NS5_{2783\text{-}2792}$, there were more antigen-specific T cells that produced IFNγ and/or TNFα in the isotype treated mice than mice treated with agonistic anti-OX40, agonistic anti-GITR, or both agonistic anti-OX40 and anti-GITR. However, mice treated with agonistic anti-GITR or both agonistic anti-OX40 and anti-GITR had more antigen-specific $CD8^+$ T cells that produced Granzyme B when compared to the isotype treated mice. Based on these findings, engaging OX40 and GITR in activated $CD8^+$ T cells could have an effect of favoring production of Granzyme B over IFNγ and TNFα. For Tfh cells, there was no difference in the frequency and number of antigen-specific cells between all four treatment groups, possibly because the cytokine production of $CD4^+$ T cells was already reduced.

The findings of this study conclude that TNFR superfamily members play an important role in T cell activation during a primary ZIKV infection. Knowledge regarding the roles TNFR superfamily members play in the adaptive immune system, particularly in regard to sustaining populations of activated T cells, will be important in developing new treatments for acute viral infections. Currently, there is no vaccine or anti-viral therapy available to treat ZIKV infections. OX40 and GITR are potential candidates for triggering the antigen-specific T cell response against ZIKV, but more research needs to be done to examine any pathogenic effects engaging

OX40 and GITR may have. Additionally, further research regarding the upregulation of Granzyme B in $CD8^+$ T cells after engagement with OX40 and GITR along with any downstream effects on survival is warranted. Performing the same investigation but using a mouse-adapted strain of ZIKV as opposed to a clinically-isolated ZIKV strain like SD001 would also be a potential avenue of research. Further testing of models that block the Type I Interferon response combined with engagement of OX40 and GITR will provide vital knowledge in understanding the T cell response against flaviviruses.

## Methods

### Virus

A clinically-isolated strain of ZIKV known as SD001 was proliferated in C6/36 *Aedes albopictus* cells (ATCC® CRL-1660™). Viral titers were determined via focus-forming assay (FFA) using baby hamster kidney (BHK)-21 cells purchased from the American Type Culture Collection (ATCC).

### Mouse experiments and virus infections

Wild-type (WT) C57BL/6J and human STAT2 knock-in (*huSTAT2* KI) mice were bred at the La Jolla Institute for Immunology in a pathogen-free facility. All infections were done using the ZIKV SD001 strain. WT mice were treated with an Ifnar1-blocking monoclonal antibody MAR1-5A3 (purchased from BioXCell, USA) one day before infection with ZIKV SD001. MAR1-5A3 was injected via an IP route at a dose of 1 mg/mouse. WT C57BL/6J mice that received MAR1-5A3 were infected via an intra-footpad route with $1 \times 10^3$ FFU of ZIKV SD001 in 20 μL of PBS with 10% FBS. WT C57BL/6J mice that did not receive MAR1-5A3 and *huSTAT2* KI mice were infected via an intra-footpad route with $1 \times 10^5$ FFU of ZIKV SD001 in 20 μL of PBS with 10% FBS. For collection of expression data of TNFR superfamily members, WT C57BL/6J mice treated with MAR1-5A3 were sacrificed at 0, 3, 5, 7, and 9 days post infection (dpi); WT C57BL/6J mice that did not receive MAR1-5A3 were sacrificed at 0, 5, and 7 dpi and *huSTAT2* KI mice were sacrificed at 0, 3, 5, and 7 dpi.

For the T cell kinetics experiment, WT C57BL/6J mice were infected via an intra-footpad route with $1 \times 10^5$ FFU of ZIKV SD001 in 20 μL of PBS with 10% FBS. 2 hours after infection mice were treated with either 200 μg of agonistic anti-OX40 (clone: OX86, BioXCell, USA), 200 μg of agonistic anti-GITR (clone: DTA-1, BioXCell, USA), both agonistic anti-OX40 at a dose of 100 μg and anti-GITR at a dose of 100 μg, or 100 μg of the isotype control for the anti-OX40 antibody(rat IgG1, κ, BioXCell, USA) and 100 μg of the isotype control for the anti-GITR antibody (rat IgG2b, BioXCell, USA). Mice were sacrificed at 7 dpi and the spleens were harvested.

### Cell isolation and flow cytometry

For extracellular staining, spleens were collected from each mouse in 10% FBS/RPMI and passed through a 70 μm cell strainer. Isolated splenocytes were plated as

$2 \times 10^6$ splenocytes/well in a volume of 100 μL into a 96-well round-bottom plate. Cells were stained with anti-CD49d FITC (BioLegend, Clone R1-2), anti-CD4 BV711 (BioLegend, Clone RM4-5), anti-CD8 BV650 (BioLegend, Clone 53-6.7), anti-CD3 PerCPCy 5.5 (BioLegend, Clone 17A2), anti-CD45 AF700 (BioLegend, Clone 30-F11), anti-CD11a PE (BioLegend, Clone M17/4), anti-OX40 BV421 (BioLegend, Clone OX86), anti-CD30 APC (BioLegend, Clone mCD30.1), anti-41BB PE-Cy7 (Invitrogen, Clone 4B4), anti-TNFR1 APC (BioLegend, Clone 55R-286), anti-BAFFR APC (eBioscience, Clone eBio7H22-E16), anti-GITR BV421 (BD BioSciences, Clone DTA-1), and anti-ICOS BV785 (BioLegend, Clone C398.4A). Tfh cells from the T cell kinetics experiment were stained with anti-CD3 PE-Cy7 (Tonbo, Clone 145-2C11), anti-CD4 APC-eFluor780 (Invitrogen, Clone GK1.5), anti-CD44 BV785 (BioLegend, Clone IM7), anti-CD62L AF700 (BioLegend, Clone MEL-14), anti-CXCR5 Biotin (BioLegend, Clone L138D7), and anti-PD1 BV605 (BioLegend, Clone 29F.1A12); twenty minutes later a secondary stain of Streptavidin-Brilliant Violet 421(BioLegend) was added. Extracellular staining was followed by fixation using BD Cytofix/Cytoperm and samples were acquired on the LSR-Fortessa (BD Biosciences). Samples were analyzed using FlowJo Software X 10.0.7 (Tree Star).

For intracellular staining, spleens were collected from each mouse in 10% FBS/RPMI and passed through a 70 μm cell strainer. Isolated splenocytes were resuspended in 10% FBS/RPMI media at $40 \times 10^6$ cells/mL, then plated as $2 \times 10^6$ splenocytes/well in a volume of 50 μL into a 96-well round-bottom plate. For activation of $CD4^+$ T cells, splenocytes were stimulated with ZIKV-specific epitopes $NS4B_{2480\text{-}2494}$ and $E_{644\text{-}658}$. For activation of $CD8^+$ T cells, splenocytes were stimulated with ZIKV-specific epitopes $E_{294\text{-}302}$ and $NS5_{2783\text{-}2792}$. Positive (PMA-Ionomycin, Invitrogen, U.S.A.) and negative (10% FBS/RPMI media) controls were used, and cells were stimulated in the presence of Brefeldin A for 6 hours. After stimulation, $CD4^+$ T cells were stained with anti-CD3 PerCPCy5.5 (Tonbo, Clone 145-2C11), anti-CD4 APC-eFluor780 (Invitrogen, Clone GK1.5), anti-CD11a PE (BioLegend, Clone M17/4), anti-CD49d BV605 (BD Biosciences, Clone R1-2), anti-IFNγ FITC (Tonbo, Clone XMG1.2), anti-IL-2 BV711 (BioLegend, Clone JES6-5H4), and anti-TNFα APC (eBioscience, Clone MP6-XT22). $CD8^+$ T cells were stained with anti-CD8 BV510 (BioLegend, Clone 53-6.7), anti-CD3 PE-Cy7 (Tonbo, Clone 145-2C11), anti-CD11a PE (BioLegend, Clone M17/4), anti-IFNγ FITC (Tonbo, Clone XMG1.2), anti-TNFα APC (eBioscience, Clone MP6-XT22), and anti-Granzyme B PE-Cy7 (eBioscience, Clone NGZB). Intracellular staining was followed by fixation using BD Cytofix/Cytoperm and buffer wash using BD PermWash. Samples were acquired on the LSR-Fortessa (BD Biosciences) and analyzed using FlowJo Software X 10.0.7 (Tree Star).

## References


1. McNeil, C.J. and A.K. Shetty, *Zika Virus: A Serious Global Health Threat.* J Trop Pediatr, 2017. **63**(3): p. 242-248.
2. Wikan, N. and D.R. Smith, *Zika virus: history of a newly emerging arbovirus.* Lancet Infect Dis, 2016. **16**(7): p. e119-e126.
3. Marchette, N.J., R. Garcia, and A. Rudnick, *Isolation of Zika virus from Aedes aegypti mosquitoes in Malaysia.* Am J Trop Med Hyg, 1969. **18**(3): p. 411-5.
4. Hussain, A., et al., *A Comprehensive Review of the Manifestations and Pathogenesis of Zika Virus in Neonates and Adults.* Cureus, 2018. **10**(9): p. e3290.
5. Mead, P.S., et al., *Zika Virus Shedding in Semen of Symptomatic Infected Men.* N Engl J Med, 2018. **378**(15): p. 1377-1385.
6. Duffy, M.R., et al., *Zika virus outbreak on Yap Island, Federated States of Micronesia.* N Engl J Med, 2009. **360**(24): p. 2536-43.
7. Cao-Lormeau, V.M., et al., *Zika virus, French polynesia, South pacific, 2013.* Emerg Infect Dis, 2014. **20**(6): p. 1085-6.
8. Hsieh, Y.H., *Temporal patterns and geographic heterogeneity of Zika virus (ZIKV) outbreaks in French Polynesia and Central America.* PeerJ, 2017. **5**: p. e3015.
9. Magalhaes-Barbosa, M.C., et al., *Trends of the microcephaly and Zika virus outbreak in Brazil, January-July 2016.* Travel Med Infect Dis, 2016. **14**(5): p. 458-463.
10. Yuki, N. and H.P. Hartung, *Guillain-Barre syndrome.* N Engl J Med, 2012. **366**(24): p. 2294-304.
11. Locksley, R.M., N. Killeen, and M.J. Lenardo, *The TNF and TNF receptor superfamilies: integrating mammalian biology.* Cell, 2001. **104**(4): p. 487-501.
12. Ward-Kavanagh, L.K., et al., *The TNF Receptor Superfamily in Co-stimulating and Co-inhibitory Responses.* Immunity, 2016. **44**(5): p. 1005-19.
13. Harigai, M., et al., *Ligation of CD40 induced tumor necrosis factor-alpha in rheumatoid arthritis: a novel mechanism of activation of synoviocytes.* J Rheumatol, 1999. **26**(5): p. 1035-43.
14. Daridon, C., et al., *Aberrant expression of BAFF by B lymphocytes infiltrating the salivary glands of patients with primary Sjogren's syndrome.* Arthritis Rheum, 2007. **56**(4): p. 1134-44.
15. Moutsopoulos, H.M., *Sjogren's syndrome: autoimmune epithelitis.* Clin Immunol Immunopathol, 1994. **72**(2): p. 162-5.
16. Battaglia, E., et al., *Expression of CD40 and its ligand, CD40L, in intestinal lesions of Crohn's disease.* Am J Gastroenterol, 1999. **94**(11): p. 3279-84.
17. Buchan, S.L., A. Rogel, and A. Al-Shamkhani, *The immunobiology of CD27 and OX40 and their potential as targets for cancer immunotherapy.* Blood, 2018. **131**(1): p. 39-48.
18. Aspeslagh, S., et al., *Rationale for anti-OX40 cancer immunotherapy.* Eur J Cancer, 2016. **52**: p. 50-66.
19. Croft, M., *The role of TNF superfamily members in T-cell function and diseases.* Nat Rev Immunol, 2009. **9**(4): p. 271-85.
20. Martinet, O., et al., *Immunomodulatory gene therapy with interleukin 12 and 4-1BB ligand: long-term remission of liver metastases in a mouse model.* J Natl Cancer Inst, 2000. **92**(11): p. 931-6.
21. Croft, M. and R.M. Siegel, *Beyond TNF: TNF superfamily cytokines as targets for the treatment of rheumatic diseases.* Nat Rev Rheumatol, 2017. **13**(4): p. 217-233.
22. Sedy, J.R., P.G. Spear, and C.F. Ware, *Cross-regulation between herpesviruses and the TNF superfamily members.* Nat Rev Immunol, 2008. **8**(11): p. 861-73.
23. Kumar, A., W. Abbas, and G. Herbein, *TNF and TNF receptor superfamily members in HIV infection: new cellular targets for therapy?* Mediators Inflamm, 2013. **2013**: p. 484378.
24. Wang, C. and T.H. Watts, *Maintaining the balance: costimulatory TNFRs and control of HIV.* Cytokine Growth Factor Rev, 2012. **23**(4-5): p. 245-54.

25. Fletcher, N.F., et al., *TNF superfamily members promote hepatitis C virus entry via an NF-kappaB and myosin light chain kinase dependent pathway.* J Gen Virol, 2017. **98**(3): p. 405-412.
26. Moreno-Cubero, E., et al., *According to Hepatitis C Virus (HCV) Infection Stage, Interleukin-7 Plus 4-1BB Triggering Alone or Combined with PD-1 Blockade Increases TRAF1(low) HCV-Specific CD8(+) Cell Reactivity.* J Virol, 2018. **92**(2).
27. Ware, C.F. and J.R. Sedy, *TNF Superfamily Networks: bidirectional and interference pathways of the herpesvirus entry mediator (TNFSF14).* Curr Opin Immunol, 2011. **23**(5): p. 627-31.
28. Steinberg, M.W., T.C. Cheung, and C.F. Ware, *The signaling networks of the herpesvirus entry mediator (TNFRSF14) in immune regulation.* Immunol Rev, 2011. **244**(1): p. 169-87.
29. Sedy, J.R., et al., *CD160 activation by herpesvirus entry mediator augments inflammatory cytokine production and cytolytic function by NK cells.* J Immunol, 2013. **191**(2): p. 828-36.
30. Grant, A., et al., *Zika Virus Targets Human STAT2 to Inhibit Type I Interferon Signaling.* Cell Host Microbe, 2016. **19**(6): p. 882-90.
31. Kumar, A., et al., *Zika virus inhibits type-I interferon production and downstream signaling.* EMBO Rep, 2016. **17**(12): p. 1766-1775.
32. Paterson, D.J., et al., *Antigens of activated rat T lymphocytes including a molecule of 50,000 Mr detected only on CD4 positive T blasts.* Mol Immunol, 1987. **24**(12): p. 1281-90.
33. Croft, M., *Control of immunity by the TNFR-related molecule OX40 (CD134).* Annu Rev Immunol, 2010. **28**: p. 57-78.
34. Nocentini, G., et al., *A new member of the tumor necrosis factor/nerve growth factor receptor family inhibits T cell receptor-induced apoptosis.* Proc Natl Acad Sci U S A, 1997. **94**(12): p. 6216-21.
35. Kwon, B., et al., *Identification of a novel activation-inducible protein of the tumor necrosis factor receptor superfamily and its ligand.* J Biol Chem, 1999. **274**(10): p. 6056-61.
36. Gurney, A.L., et al., *Identification of a new member of the tumor necrosis factor family and its receptor, a human ortholog of mouse GITR.* Curr Biol, 1999. **9**(4): p. 215-8.
37. Ronchetti, S., et al., *GITR, a member of the TNF receptor superfamily, is costimulatory to mouse T lymphocyte subpopulations.* Eur J Immunol, 2004. **34**(3): p. 613-622.
38. Chiang, H.S. and H.M. Liu, *The Molecular Basis of Viral Inhibition of IRF- and STAT-Dependent Immune Responses.* Front Immunol, 2018. **9**: p. 3086.
39. Ashour, J., et al., *NS5 of dengue virus mediates STAT2 binding and degradation.* J Virol, 2009. **83**(11): p. 5408-18.
40. Dar, H.A., et al., *Structural analysis and insight into Zika virus NS5 mediated interferon inhibition.* Infect Genet Evol, 2017. **51**: p. 143-152.
41. Weinberg, A.D., et al., *Engagement of the OX-40 receptor in vivo enhances antitumor immunity.* J Immunol, 2000. **164**(4): p. 2160-9.
42. Pardee, A.D., et al., *A therapeutic OX40 agonist dynamically alters dendritic, endothelial, and T cell subsets within the established tumor microenvironment.* Cancer Res, 2010. **70**(22): p. 9041-52.
43. Burocchi, A., et al., *Intratumor OX40 stimulation inhibits IRF1 expression and IL-10 production by Treg cells while enhancing CD40L expression by effector memory T cells.* Eur J Immunol, 2011. **41**(12): p. 3615-26.
44. Murphy, K.A., et al., *An in vivo immunotherapy screen of costimulatory molecules identifies Fc-OX40L as a potent reagent for the treatment of established murine gliomas.* Clin Cancer Res, 2012. **18**(17): p. 4657-68.
45. Ramirez-Montagut, T., et al., *Glucocorticoid-induced TNF receptor family related gene activation overcomes tolerance/ignorance to melanoma differentiation antigens and enhances antitumor immunity.* J Immunol, 2006. **176**(11): p. 6434-42.
46. Leyland, R., et al., *A Novel Murine GITR Ligand Fusion Protein Induces Antitumor Activity as a Monotherapy That Is Further Enhanced in Combination with an OX40 Agonist.* Clin Cancer Res, 2017. **23**(13): p. 3416-3427.

47. Ko, K., et al., *Treatment of advanced tumors with agonistic anti-GITR mAb and its effects on tumor-infiltrating Foxp3+CD25+CD4+ regulatory T cells.* J Exp Med, 2005. **202**(7): p. 885-91.